9th International Conference on NDT of Art, Jerusalem Israel, 25-30 May 2008
For more papers of this publication click: www.ndt.net/search/docs.php3?MainSource=65

NON-DESTRUCTIVE NEUTRON DIFFRACTION STUDY OF INTERNAL STRUCTURE OF ARCHAEOLOGICAL METAL ARTIFACTS FROM ISRAEL✡

El'ad N. Caspi,[1] Oleg Rivin,[1] Hanania Ettedgui,[1]
Martin Peilstöcker[2] Sana Shilstein,[3] Sariel Shalev[3,4]
[1]Physics Department, Nuclear Research Centre – Negev,
PO Box 9001, 84190 Beer-Sheva, Israel
[2]Israel Antiquities Authority, PO Box 1230, 61012 Tel Aviv, Israel
[3]Kimmel Center for Archaeological Sciences,
Weizmann. Institute of Science, 76100 Rehovot, Israel
[4]Leon Recanati Inst. for Maritime Studies & Inst. of Archaeology,
University of Haifa, Mount Carmel, 31905 Haifa, Israel

ABSTRACT

Neutron diffraction (ND) analyses of ancient metals show that this method is capable of detecting differences in the inner composition and microstructure of ancient metal objects. This gives archaeometallurgists a powerful non-destructive tool to help generate a better understanding of ancient modes of production (i.e. casting direction and mechanical and thermal treatment of selected parts of the original cast). Introducing this method in Israel will allow us to study unique and precious archaeological metal artifacts that cannot be taken abroad or cut or drilled for sampling. We carried out ND measurements on two Middle Bronze Age I "Eye" axes, one made of bronze and the other of silver, both found recently in the ancient cemetery of Mahzevat Shuni. Both artefacts are rare finds with the silver axe unique in the archaeology of Israel. ND was carried out on the newly assembled KARL diffractometer at the IRR-1 at the Nuclear Research Center – Soreq, Israel. Preliminary results confirmed our ability to clearly identify and analyze metal compositions and phases, and obtain information on the texture of the studied alloy. In particular, ND measurement on the bronze axe revealed the existence of three copper-tin phases, among which two are bronze phases with different copper/tin ratio and the third is the γ-bronze phase. Unlike the bronze axe, the silver axe diffraction show the existence of only one silver/copper phase. Our ND data is discussed in comparison with XRF surface measurements which combined with the ND data can shed light on the in-depth material composition profile.

INTRODUCTION

In the summer of 2001 during the IAA excavations of a Middle Bronze Age cemetery in 'Enot Shuni' [1] near the coast of the Mediterranean some 55 Kilometers north of modern Tel Aviv in Israel, two rare battle axes were found. The axes were unearthed in tomb 59 and in tomb 79 (Nos. 50037, 7300 respectively, Fig. 1) from the Intermediate Bronze Age (I.B.) – early Middle Bronze Age (M.B.IIa), and therefore are dated to the 21st – 20th century B.C. The bronze axe (No 7300) measures 11,7cm (shaft), 7.5cm (max width) with an opening of 3 x 4.2 cm and an opening of 3 x 4.3 cm. The oval shaft varies from 2 x 1cm on one side to 2.5 x 1.5cm on the other. The silver axe (No 50037) measures 9.2cm (shaft), 7.5cm (width), 2.5 x 3.8cm and 2.5 x 3.9cm (openings) and 1.5 x 2cm to 1.8 x 2.6cm (shaft).

Fig. 1 – A photos of the (a) bronze axe (No. 7300) and (b) silver axe (No. 50037).

ARCHAEOMETALLURGICAL BACKGROUND

During the EB-MB period in the southern Levant fenestrated metal battle axes in the shape of an 'eye axe' (*i.e.* Ref. [2]) were found mainly in burials and in hoards associated with sacred places in Syria – Palestine and Iran. Single similar objects were found all over the ancient Near East from Anatolia in the north to Mesopotamia in the East and Egypt in the South-West. (op. cit. [3]). An intact double stone mold for casting such axes was found in the tomb of 'seigneur aux caprides' in Ebla, Syria with two bronze fenestrated axes that were probably cast in different mold as could be seen from their cast 'vein' like decoration [4]. The stone mold show that this type of axe was cast with no runners or risers and the metal was poured into the mold from a sprue attached to the center of the blade. A cylinder core (not found,

maybe made of clay and disposed after each cast) was inserted at the base of the stone mold for creating the hollow socket of the axe. Thin scratches in the mold on both sides of the sprue were used as venting channels for gasses to escape during casting process for ensuring a smooth and solid cast. Three small holes (one at the bottom and two on both sides of the upper side) were used to insert small wooden pegs for ensuring the exact fitting the two mold pieces before casting. After casting the stone mold was opened, the clay core was removed and the blade was cleaned and polished from the sprue metal fill and the remains of metal that might enter the venting channels. Most of the axe body was left as cast, leaving surface cast decoration around the 'eyes' and the solid area of the blade.

Due to the rarity of these artifacts and their fragile and corroded condition the routine methods for their archaeometallurgical study (i.e. cut section with preserved solid metal for optical and electron microscopy metallography and/or drilled sample for metal compositional analysis etc.) were not feasible. Therefore a different research program was defined using non-destructive XRF analyses of the corroded cleaned surfaces of these 'museum pieces' and neutron diffraction analyses of their mass volume. In this research we aimed at seeing 'behind' the surface corrosion composition by 'entering' into the mass body of the artifacts with neutrons for 'seeing' by analyzing their diffraction, the volume of the preserved metal and if it was left as-cast or was mechanically and/or thermally treated after casting and if so – to what extend it was homogenized by heating and hammered and annealed.

EXPERIMENTAL CONDITIONS

Room temperature neutron diffraction (ND) measurements were carried out on the KARL diffractometer in the IRR-1 at Soreq Research Centre. Neutrons from the reactor were monochromatized using a pyro-graphite monochromator, resulting in a 2.421 Å neutron beam. The multi-detector (bank of 14 ^{3}He detectors with angle step 3.5^{0}) was used for registration the ND pattern in the scattering angle range of $2\theta=20^{o}–120^{o}$. ND data were collected separately from the middle and blade parts of both copper and silver axes, and also from pure (3N) silver and copper powders as standards. The primary beam formed by Cd apertures had the sizes 10 mm x15 mm for the middle part of each axe, and the sizes 10 mm x 10 mm for the blade part. ND data are analyzed using the Rietvled refinement analysis with the FULLPROF program [5]. The Thompson-Cox-Hastings pseudo-Voigt function was used for peak shape description [6]. We used a simple Gaussian fit [7] of the copper to determine the width of the diffraction lines.

For XRF analysis of the axes a bench top model EX-310LC (Jordan Valley Co) was used [8]. For weakening the influence of corrosion the tested part of the sample surface was slightly cleaned mechanically. The conditions used for the analysis where 35 kV of a rhodium tube and a primary beam size of 2 mm in diameter. For each surface 2-3 points were measured and the results were averaged. Taking into account the influence of corrosion – the accuracy is about 10%.

RESULTS OF XRF ANALYSIS AND ND ANALYTICAL DATA

The results of the XRF analysis show that one axe (No 7300) was made of copper alloyed with tin i.e. bronze (Cu + 5.5%Sn) and the other axe (No. 50037) was made of silver alloyed with copper (Ag + 23%Cu in the corrosion layer). The results represent corroded surface layers of about 10 microns in depth.

Bronze Axe (No. 7300)

On the ND patterns of the copper powder and the middle and blade part of the bronze axe (Fig. 2) the strongest lines are identified as {111} and {200} of a face-centered cubic lattice with cell parameters in the range of 3.64 – 3.68 Å, in agreement with the data for the lattice type and the unit cell parameters of copper element [9] and copper – tin bronze [10]. It means that the bronze axe contains mainly the Cu – Sn solid solution with cell parameter increased in comparison with pure copper (Table 1). This increasing of the cell parameter is caused by substitution of copper atoms in the lattice by the bigger tin atoms.

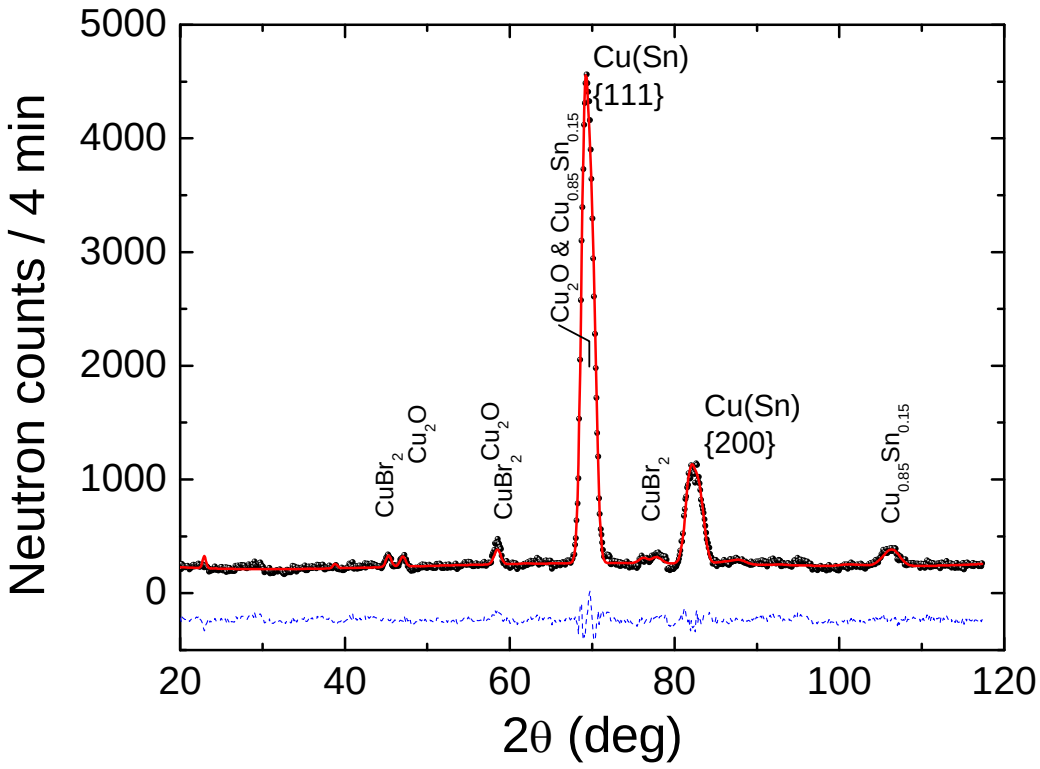

Fig. 2 – Rietveld refinement analysis of the ND data taken from the middle part of the copper axe. Solid circles, continuous line and dashed line are measured data, refined model and the difference between them, respectively. The refined model includes two Cu – Sn solid solutions along with 3 additional impurity phases, of which the strongest lines are indicated in the graph.

Obviously, lines in the diffraction patterns deduced from both parts of the bronze axe are significantly wider than the corresponding line widths of the copper powder (Fig. 3, Table 2). Such a situation is typical for inhomogeneous solid solutions with composition varied from one part of the object to the other. For describing this solution we used the model, where two bronze phases were introduced with different cell parameters, representing two different tin percentages in the bronze (Fig. 3). As result we received two values of the tin concentration – about 5% $(Cu – Sn)_1$ and 12% $(Cu – Sn)_2$. These results are similar for both part of this axe (Table 1). A small decrease in the lattice constant (and correspondingly in the Sn content) is observed when comparing results from the middle part of the axe to results from the blade. Yet, this change is not far from one standard deviation of the experimental method (Table 1). Therefore, we used the averaged data of the lattice constants for the determination of the Sn content.

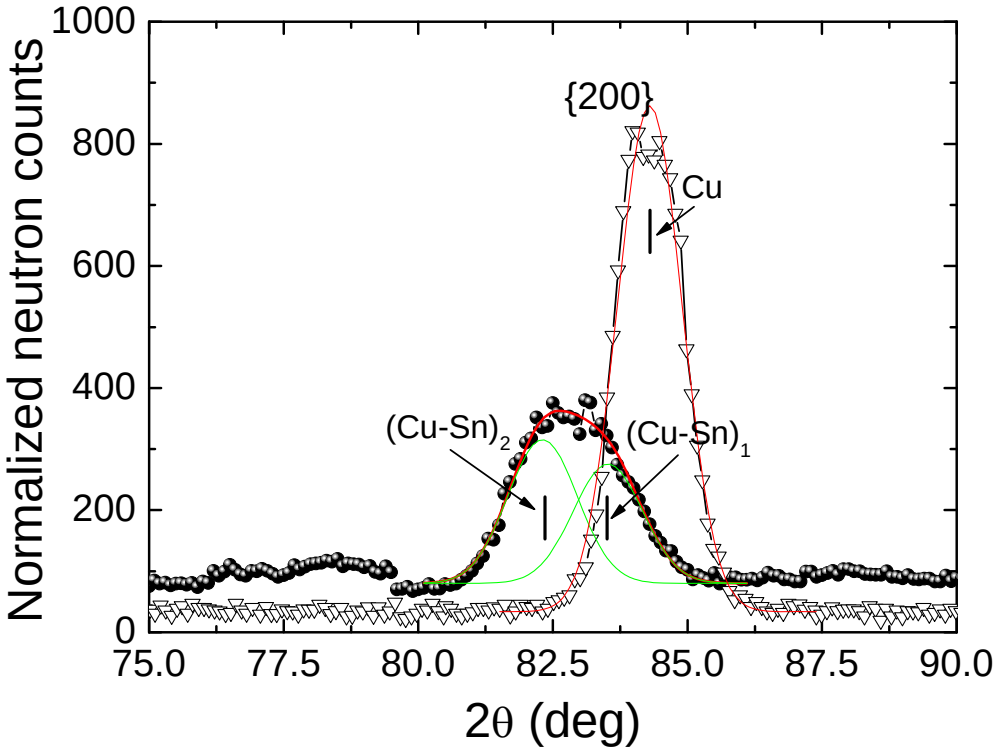

Fig. 3 – Part of the neutron diffraction pattern of the copper powder (open up-side-down triangles) and middle axe part (solid circles). A Gaussian fit to the data is also shown for both cases.

ND patterns of the middle and blade parts of the bronze axe contain several small diffraction lines in addition to the strong solid solution lines discussed above (Fig. 2). These lines belong to several impurity phases among which the body-centered cubic structure with the cell parameter a≈3.02 Å that is consistent with the $Cu_{0.85}Sn_{0.15}$ phase [11], and the $CuBr_2$ phase [12]. Additional, weaker lines, belong to the Cu_2O [13] phase. The existence of the $Cu_{0.85}Sn_{0.15}$ and Cu_2O is commonly found in bronze artifacts [10]. The $CuBr_2$ phase could be interpreted as corrosion product.

Solution	Middle part of the axe	Blade part of the axe
$(Cu – Sn)_1$	3.648(5)	3.629(5)
$(Cu – Sn)_2$	3.689(5)	3.667(5)
(Ag – Cu)	4.077(5)	4.076(5)

Table 1. The cubic lattice constants (in Å) for solid solutions found in the bronze axe and in the silver axe. Number in the parentheses is estimated error.

Object	Cu powder	Bronze	Axe	Ag powder	Silver	Axe
Part		middle	blade		middle	blade
w(111)	0.95(2)	1.40(3)	1.43(2)	0.86(3)	0.83(2)	0.85(2)
w(200)	1.31(3)	1.93(5)	1.70(4)	1.06(4)	0.93(5)	1.06(4)

Table 2. The widths, w (in degrees), of the neutron diffraction lines {111} and {200} of copper powder and bronze axe, for silver powder and silver bronze axe. Values are deduced by a single Gaussian fit to the neutron data [7].

Ag Axe (No 50037)

On the ND patterns of the silver powder and the middle and blade part of the silver axe (Fig. 4) the strongest lines are identified as (111), (200), and (220) of a face-centered cubic

structure with cell parameters in the range 4.07 – 4.09 Å, in agreement with silver element [14] and silver – copper alloy cell parameters [11]. It means that the silver axe contains mainly the solid solution with cell parameter decreased in comparison with pure silver. This decreasing of the cell parameter is caused by substitution of silver atoms in the lattice by the smaller copper atoms. Assuming limited solubility of copper in the silver metal, and the linear dependence of the lattice constant on the concentration for the solid solution (i.e. Vegard's law) 3 - 4% (atomic) or about 2% (in weight) of copper is estimated to be present in the main part of the silver axe. ND patterns of the middle and blade parts of the silver axes contain also several small diffraction lines in addition to the strong silver lines discussed above (*cf.* Fig. 4). These lines belong to several phases among which Cu is the strongest. The existence of Cu is typical for Ag – Cu alloys with Cu concentration higher than solubility limit (about 9% in weight) [11]. Additional observed phases - AgCl [16] (in both part of the silver axe), and $CuCl_2$ [17] (in the middle part only) - could be interpreted as corrosion products.

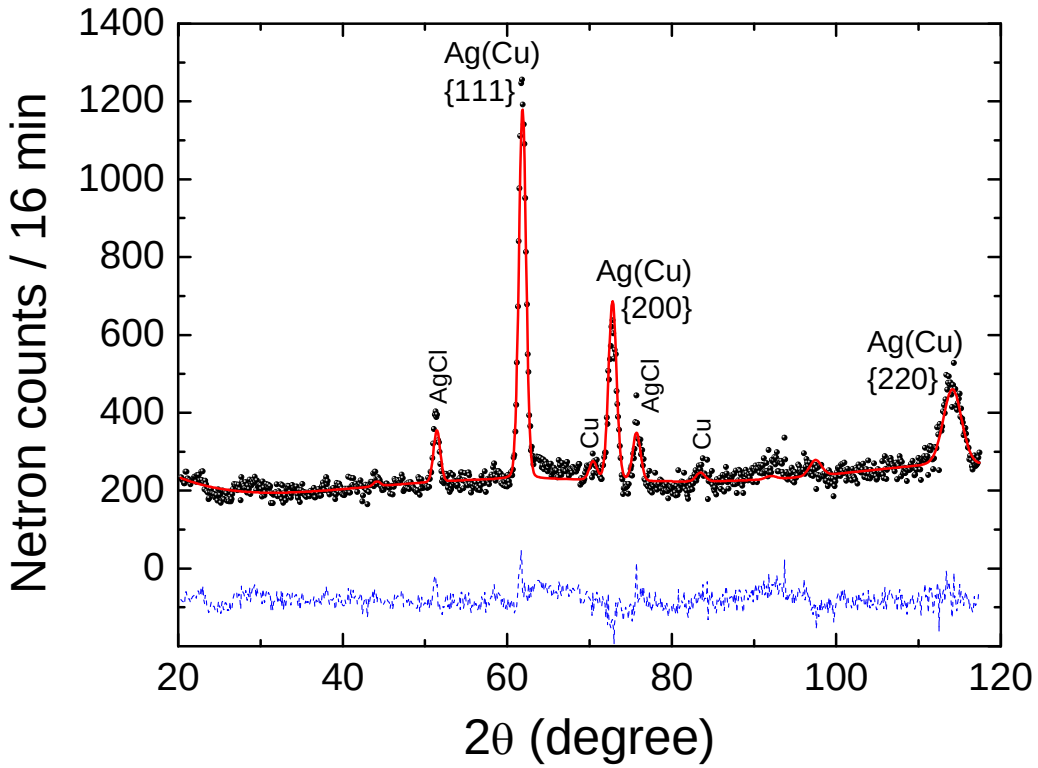

Fig. 4 – Rietveld refinement analysis of the ND data taken from the blade part of the silver axe. Solid circles, continuous line and dashed line are measured data, refined model and the difference between them, respectively. The refined model includes Ag – Cu solid solution along with 2 additional impurity phases, of which the strongest lines are indicated in the graph.

Unlike the bronze axe, the silver diffraction lines in both parts of the silver axe have similar width as the silver powder lines.

DISCUSSION AND CONCLUSIONS

The above described neutron diffraction data of object No. 7300 are similar to data of the internal structure of an as-cast non-homogeneous bronze without additional thermal and/or mechanical treatment [10]. Annealing and cold work of the blade area after casting, even if it was conducted originally could not be seen in this case due to heavy corrosion and a need of a more detailed neutron diffraction study with better space resolution (about 1 mm).

It is well known that as a result of the big difference in the melting temperatures of the Cu and Sn metals the solidification process starts from growth of grains (dendrites) containing solution of relatively poorer Sn content and end with interdendritic solidification of Sn rich solutions i.e. “dendrite liquation” [15]. For bronze casting this liquation gives the minimal Sn content close to the surface and the maximal Sn content in the bulk. From our ND results the bronze axe (No. contains two solutions (12 and 5% Sn). From our XRF data the surface layers contain 5.5% Sn. It means that the Sn rich part is placed indeed in the bulk in accordance with expected situation for bronze cast objects. The absence of any sign of treatment after casting in the silver axe No 50037 could indicate the use of this object as a ceremonial object rather then a 'real' weapon.

The solubility limit of Cu in Ag is not more than several percents. Thus, the Cu content, measured by the XRF (about 23% Cu), suggests the existence of two phases based on the Ag and Cu metals. This is in qualitative agreement with our ND data, where accurate quantitative interpretation is difficult due to the influence of corrosion products and strong neutron attenuation by silver.

The data measured in this work show no difference between the blade and middle part of both silver and bronze axes, albeit a hint that such a difference does exist in the bronze axe (please see cell parameters in table 1). A more spatially resolute ND measurement is required to more accurately determine whether a difference does exist or not. This will enable us to shed more light on the means of manufacturing the studied axes.

However, it is clear from our present preliminary relatively low resolution ND data that this method is able to easily observe the original artifact’s composition regardless of the existence of corrosion and without the need to cut or drill the object.

ACKNOWLEDGEMENTS
The authors would like to thank Hanoch Hirshfeld, Tuvia Arbel, and David Blatman for help in conducting the neutron diffraction measurements. One of us (ENC) would like to thank David Melnik for his guidance and helpful suggestions.

ENDNOTE
✡This manuscript is to be submitted for publication in Archaeometry.

BIBLIOGRAPHY
1. Matthiae P. 1993. in: Syrie Memoire et Civilisation, Institute du Monde Arabe. Pp 206.
2. Miron 1992: 51-71.
3. catalogue nos. 225-232; p.57-58.
4. Gorzalczany, A. 2005. Shuni: A New Middle Bronze IIA Domestic Site on the Northern Bank of Nahal Tannenim, Tel Aviv 32:32- 49.; Peilstöcker, M. and Sklar-Parnes, D. 2005. ‘Enot Shuni. HA-ESI 117 (electronic journal, www.hadashot-esi.org.il, 19.15.2006).
5. J. R. Carvajal, Physica B 192, 55 (1993); J. R. Carvajal, An Introduction to the program FULLPROF 2000, ver. July2001.
6. P. Thompson, D. E. Cox, J. B. Hastings, J. Appl. Crstallogr. **20**, 79 (1987).
7. $y=y_0 + (A/(w*sqrt(PI/2)))*exp(-2((x-xc)/w)^2)$
8. S.Shalev, S.Sh.Shilstein, Yu.Yekutieli, Talanta **70**, 909 (2006)
9. Landolt-Boernstein “Zahlenwerten und Funktionen aus Naturwissenschaften und Technik”, Neue Serie, K.-H.Hellwege (Ed.), Springer, Berlin – Heidelberg – New York, 1973, Gruppe 3, Band 6, Seite 7.

10. S. Siano, L.Bartoli, M.Zoppi, W.Kockelmann, W.Daymond, J.A.Dann, M.G.Garagnani, M.Miccio, Proc. Archaeometallurgy Europe **2**, 319 (2003).
11. T.B.Massalski [Ed. In Chief] Binary Alloys Phase Diagrams, 2nd Edition, ASM International, 1990.
12. See [9], Gruppe 3, Band 7, Teil a, Seite 520.
13. See [9], Gruppe 3, Band 7, Teil b2, Seite 19.
14. See [9], Gruppe 3, Band 6, Seite 1.
15. M.C. Smith “Alloy Series in Physical Metallurgy”, Harper@Brothers, New York, 1956.
16. See [9], Gruppe 3, Band 7, Teil a, Seite 357.
17. See [9], Gruppe 3, Band 7, Teil a, Seite 356.

Back to Top